

# Investigation of the possible link between LDN 288 and NGC 6494 using polarimetric observations

R. Silva<sup>1</sup>, W. Corradi<sup>1,2</sup>, N. Sasaki<sup>3</sup>, & W. Reis<sup>1,4</sup>

<sup>1</sup> Universidade Federal de Minas Gerais e-mail: rafaelx26@ufmg.br, wilsonr@fisica.ufmg.br

<sup>2</sup> Laboratório Nacional de Astrofísica e-mail: wbcorradi@lna.br

<sup>3</sup> Universidade do Estado do Amazonas e-mail: nsasaki@uea.br

<sup>4</sup> Instituto Brasileiro de Mercado de Capitais e-mail: wilson.reis@professores.ibmec.edu.br

**Abstract.** In this work, a polarimetric investigation was carried out toward the dark cloud LDN 288, which, together with the nebular object SNO 85 and the embedded cluster Ryu 10, hosts a star-forming region that was possibly triggered after the formation of the open cluster NGC 6494. GAIA DR3 reddening–distance data reveal two components along the line of sight at  $(650 \pm 50)$  pc and  $(1100 \pm 100)$  pc, where  $A_V$  increases abruptly. Polarimetric observations with SPARC4 confirm these structures through corresponding increases in polarization degree for 2 of the 9 fields analyzed.: from  $P = (1 \pm 0.5) \%$  to  $(2 \pm 0.5) \%$  at 650 pc, and an abrupt increase from  $P = (3 \pm 1)$  to  $(7 \pm 1)$  in 1100 pc. The correlation between polarization, extinction, and polarization efficiency supports the existence of these two components. Although the data establish the presence of two dust layers, it is still not possible to determine unambiguously which one corresponds to LDN 288. The results are compatible with the  $(500 \pm 200)$  pc distance of Ryu 10. In the near future we expect to complete the analysis of the remaining 7 fields to identify the true distance of LDN288 and its possible connection to the evolution of NGC6494.

**Resumo.** Neste trabalho foi feita uma investigação polarimétrica na direção da nuvem escura LDN 288, que, juntamente com o objeto nebuloso SNO 85 e o aglomerado embebido Ryu 10, abriga uma região de formação estelar possivelmente desencadeada após a formação do aglomerado aberto NGC 6494. Os dados de avermelhamento por distância do GAIA DR3 revelam duas componentes ao longo da linha de visada, em  $(650 \pm 50)$  pc e  $(1100 \pm 100)$  pc, onde  $A_V$  aumenta abruptamente. Observações polarimétricas com a SPARC4 confirmam essas estruturas por meio de aumentos correspondentes no grau de polarização para 2 dos 9 campos analisados: de  $P = (1 \pm 0.5) \%$  para  $(2 \pm 0.5) \%$  em 650 pc, e um aumento abrupto para  $P = (3 \pm 1)$  até  $(7 \pm 1)$  em 1100 pc. A correlação entre polarização, extinção e eficiência de polarização reforça a existência dessas duas componentes. Embora os dados estabeleçam a presença de duas camadas de poeira, ainda não é possível determinar inequivocamente qual delas corresponde à LDN 288. Os resultados são compatíveis com a distância de  $(500 \pm 200)$  pc do aglomerado Ryu 10. Num futuro próximo esperamos concluir a análise dos 7 campos restantes para identificar a verdadeira distância de LDN288 e sua possível conexão com a evolução de NGC6494.

**Keywords.** ISM: dark clouds – Methods: color excess per distance diagrams – Polarimetric analysis

## 1. Introduction

Multi-wavelength polarimetric observations are essential for probing the interstellar medium (ISM). Comparisons of the polarization degree and angle allows to investigate the dust distribution and alignment in the ISM (Corradi et al. 2004). It reveals the Local Bubble (Reis et al. 2011; Santos et al. 2011), surrounded by other interstellar bubbles, some linked to active star-forming regions (Reis & Corradi 2008).

LDN 288 is a  $0.05 \text{ deg}^2$  area high- opacity dark cloud listed in the Lynds' Catalogue of Dark Nebulae (Lynds 1962). It's J2000 coordinates are  $\alpha \approx 17^{\text{h}}57^{\text{m}}42.6^{\text{s}}$ ,  $\delta \approx -18^{\circ}32'27''$  and Galactic coordinates  $l \approx 10.41^{\circ}$ ,  $b \approx 2.9^{\circ}$ . The most detailed study of LDN 288 is (Gyulbudaghian & May 2006), which analyzes the peculiar object SNO 85. Ryu & Lee (2018) identified the Ryu 10 embedded cluster, placing it at a distance of  $(500 \pm 200)$  pc. Is is suspected that LDN 288 hosts a region of star formation that may have been triggered after the formation of the open cluster NGC 6494, see figure 1.

The distance of the cluster was previously estimated at  $(649 \pm 90)$  pc using Gaia DR3 (Gaia Collaboration 2023) data and an astrometric CMD decontamination method, e.g. Ferreira et al. (2020, 2025); Angelo et al. (2025). In this paper our goal is to determine the distance of LDN288 to compare both with the previous estimates of Gyulbudaghian, that places the cloud at 380–990 pc, and with the distance of NGC 6494.

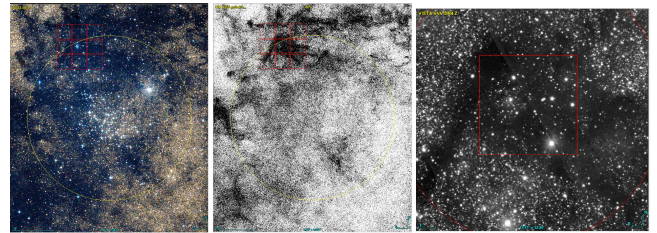


FIGURE 1: LDN 288 and NGC 6494. Left: DSS2; Middle: GAIA density map; Right: Central field in VISTA VVV-DR4-Z; The yellow circle of 30 arcmin radius is centered on the cluster, while the red area marks the SPARC4 fields of  $5.7 \times 5.7$  arcmin.

## 2. Methodology

The reduction of the data converts intensity measurements at different analyzer angles into the physical polarization parameters  $P$  and  $\theta$ . This process was performed using the SPARC4 Pipeline (Martioli et al. 2025), a Python-based set of routines designed for photometric and polarimetric data obtained with SPARC4. The pipeline was built on the ASTROPOP package (Campagnolo 2018).

The resulting polarimetric four bands data were cross-matched with the Gaia DR3 catalog, which provides accurate distances and stellar parameters derived from a statistical model

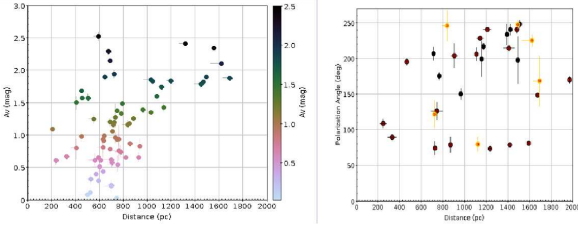


FIGURE 2: Left: Diagram of reddening as a function of distance in the direction of the LDN 288. Right: Diagram of the polarization angle as a function of distance. The stars in yellow and black are from short and long exposures, respectively.

that combines satellite measurements with prior knowledge of stellar physics and Galactic structure. The percentiles of these parameters are used to generate the uncertainties, which were included in the selection criteria for each SPARC4 channel.

The distances to the dark clouds were first determined using the classical method of reddening as a function of distance, which traces the spatial distribution of interstellar dust, e.g. (Reis & Corradi 2008; Corradi et al. 1997). Since extinction and reddening accumulate along the line of sight, the color excess is expected to be negligible for nearby stars and to increase with the amount of intervening dust. Thus,  $E(B-V)$  vs. distance diagrams were constructed for stars in the target fields to identify abrupt rises in reddening, e.g. Corradi et al. (2004), which mark the locations of dust layers and the distance to the clouds. The analysis of visual absorption  $A_V$ , polarization  $P$ , polarization angle  $\theta$  and polarization efficiency as a function of distance, provides robust evidence for the existence of polarizing components of the ISM (Serkowski 1973) and reveals interstellar magnetic field through observations of starlight polarization. ((Axon & Ellis 1976)).

### 3. Discussion and Results

The reddening–distance diagram (figure 2), constructed from stars detected within the central field, shows a first significant rise in  $A_V$  at  $(650 \pm 50)$  pc, a second increase at  $(1100 \pm 100)$  pc, and a broader dust layer is suggested beyond  $(1500 \pm 50)$  pc.

Although the g band provided few usable stars due to selection criteria (see figures 3 e 4), the r, i, and z bands yielded consistent results. In the z band — where more stars penetrate the cloud — polarization angles cluster around  $100^\circ$  for  $d < 650$  pc. At larger distances, they separate into two preferred orientations near  $75^\circ$  and  $225^\circ$ , see figure 2.

Polarization–distance diagrams (figure 3) for the central field reveal two main components. The first occurs at  $(650 \pm 50)$  pc, where the polarization degree rises from  $P = (1 \pm 0.5)\%$  to  $(2 \pm 0.5)\%$ . The second appears near  $(950 \pm 50)$  pc, with a sharp increase to  $P = (3-7)\%$ .

The polarization efficiency diagram ( $P/A_V$ ) supports a well-defined component at  $(650 \pm 50)$  pc, and the correspondence between jumps in  $A_V$  and  $P$  indicates physically distinct dust layers containing magnetically aligned grains, see figure 4. Thus, the first component is identified as the distance to LDN 288. The distance obtained here is more precise and significantly narrower range (380- 990 pc) reported by (Gyulbudaghian & May 2006). It is also compatible, within uncertainties, with the distance of  $(500 \pm 200)$  pc estimated by (Ryu & Lee 2018) for the embedded cluster Ryu 10, suggesting that LDN 288 may belong to the same large-scale structure. A map of the polarization of the two analyzed fields is shown in the figure 5.

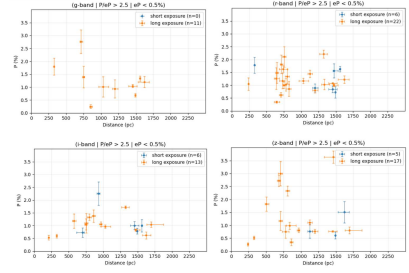


FIGURE 3: Spectral dependence of  $P$  as a function of distance. These diagrams show that the structure of LDN 288, between 600 and 700 pc, is being affected by dust grains.

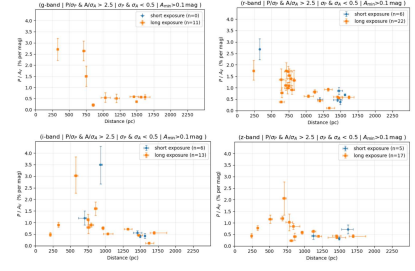


FIGURE 4: Spectral dependence of polarization efficiency,  $P/A_V$ , as a function of distance.

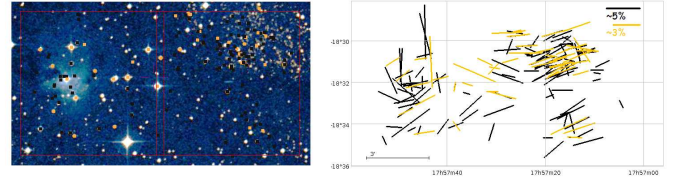


FIGURE 5: Left: Region delimited by two observed fields in the direction of LDN 288. Right: Polarization map of these fields.

### 4. Conclusions

This new determination, using polarimetric data of the dark cloud LDN288, indicates that it is located at  $(650 \pm 50)$  pc. This value constrains the measurements performed by Gyul'budagyan and further strengthens the physical association between LDN288 and the open cluster NGC6494, which is at a calculated distance of  $(649 \pm 90)$  pc.

*Acknowledgements.* W.Corradi acknowledges the support from CNPq - BRICS 440142/2022-9, FAPEMIG APQ 02493-22 and FNDCT/FINEP/REF 0180/22.

### References

- Angelo, M. S., Santos, J. F. C., et al. 2025, MNRAS, 539, 2513
- Axon, D. J. & Ellis, R. S. 1976, MNRAS, 177, 499
- Campagnolo, J. C. N. 2018, ASCL, ascl:1805.024
- Corradi, W. J. B. et al. 1997, A&A, 326, 1215
- Corradi, W. J. B. et al. 2004, A&A, 347, 4
- Ferreira, F. A., Santos, J. F. C., et al. 2020, MNRAS, 496, 2021
- Ferreira, F. A., Corradi, W. J. B., et al. 2025, MNRAS, 539, 265
- Gaia Collaboration 2023, A&A, 674, A41
- Gyulbudaghian, A. L. & May, J. 2006, Ap, 49, 530
- Lynds, B. T. 1962, ApJS, 7, 1
- Martíoli, E., Rodrigues, C. V., et al. 2025, Bol. Soc. Astron. Bras., 36, 65
- Reis, W. & Corradi, W. J. B. 2008, A&A, 486, 471
- Reis, W., Corradi, W. J. B., Aveliz, M. A., & Santos, F. P. 2011, ApJ, 734, 8
- Ryu, J. & Lee, M. G. 2018, ApJ, 856, 152
- Santos, F. P., Corradi, W. J. B., & Reis, W. 2011, ApJ, 728, 104
- Serkowski, K. 1973, IAUS, 52, 145